

(200)
R290
no. 98-135
c. 1

Mapat: m(200)
R290
no. 98-135

DEPARTMENT OF THE INTERIOR
U.S. GEOLOGICAL SURVEY

Geologic Map of Akutan Island, Alaska

By

Donald H. Richter, Christopher F. Waythomas, Robert G. McGimsey,
and Peter L. Stelling

Open-File Report 98-135



This report is preliminary and has not been reviewed for conformity with the
North American Stratigraphic Code

Alaska Volcano Observatory
Anchorage, Alaska
1998

U.S. DEPARTMENT OF THE INTERIOR
BRUCE BABBITT, Secretary

U.S. GEOLOGICAL SURVEY
Thomas J. Casadevall, Acting Director

For additional information:

U.S. Geological Survey
Alaska Volcano Observatory
4200 University Drive
Anchorage, AK 99508

www.avo.alaska.edu

Copies of this report may be purchased from:

U.S. Geological Survey
Branch of Information Services
Box 25286
Denver, CO 80225-0286

CONTENTS

Geologic note	1
Acknowledgements	2
References	3
Description of map units	15

FIGURES

1. Oblique aerial view of Akutan Volcano and eastern part of Akutan Island from the west	4
2. Detailed sketch map of Akutan caldera as of July 1996.	5
3. Variation diagrams for volcanic rocks from Akutan Island	6
4. Map of Akutan Island showing location and size of lithic volcanic bombs from assumed caldera forming eruption	7

TABLES

1. Chemical analyses of volcanic rocks from Akutan Island	8
2. Radiocarbon dates associated with tephra assumed to be product of Akutan caldera formation	12
3. $^{40}\text{Ar}/^{39}\text{Ar}$ ages of volcanic rocks from Akutan Island	13

Geologic Map of Akutan Island, Alaska

By Donald H. Richter¹, Christopher F. Waythomas¹, Robert G. McGimsey¹,
and Peter L. Stelling²

GEOLOGIC NOTE

Akutan Island, approximately 29 km long by 21 km wide, is the largest island in the Krenitzin group in the eastern part of the Aleutian arc. The island is dominated by Akutan Volcano, one of the most active volcanoes in the Aleutian arc (fig. 1). At least 27 separate volcanic events have occurred since 1790 and it is likely that other activity has gone unrecorded because of the remoteness of the island (Miller and others, 1998).

Lava flows and pyroclastic and volcaniclastic deposits from both the modern Akutan stratocone and an ancestral cone cover much of the western half of the island. The eastern half of the island is composed of older (1.5-3.3 Ma) layered volcanic rocks from several different sources. Many are probably from an ancestral Akutan volcano; however, some sources were apparently volcanic centers that were largely offshore the present island. Lava flows in this older sequence below about 1,000 feet (300 m) in elevation were emplaced subaqueously and subaerially above 1,000 feet (300 m), indicating a major lowering of sea level in the late Pliocene (Haq and others, 1987). This distinction between subaerial and subaqueous has been used recently to distinguish two informal volcanic units on the island: the Hot Springs Bay volcanics and the Akutan volcanics (Swanson and Romick, 1988; Romick and others, 1990; Romick, 1991). The present study does not support entirely different sources for the two volcanic units, and we suggest these names be abandoned.

Modern Akutan Volcano contains a 2-km-wide summit caldera with a 140-m-high intracaldera cone, which has been the site of all documented historic eruptive activity (fig. 2). During the last major eruption in 1978, lava issuing from this cone covered a large part of the caldera floor, flowed through a gap in the northwest caldera wall, and flowed down the north flank of the stratocone to within 2 km of the ocean. Evidence from tephra and lahar stratigraphy and from tephra, bomb, and lava composition suggests that the modern caldera formed about 1611 years B.P. during a major Strombolian or sub-Plinian eruption. About 2 km southwest of the present caldera, remnants of an older caldera wall, probably of late Pleistocene age, crop out through the extensive tephra and lahar deposits that mantle Akutan's summit area. The entire modern cone, including the older caldera, has probably been constructed during the past 500,000 years. Extensive subaerial lava flows, as old as 1.4 Ma, from an ancestral Akutan volcano dip away from the modern Akutan cone area.

At least four large eruptive centers are recognized peripheral to the modern Akutan cone. The youngest center, which produced the Lava Point flows and cone at the northwest tip of the island, may be historic (younger than about A.D. 1800) in age. Cascade Bight eruptive center, southeast of the Akutan cone, includes a small lava flow, dated at 0.15 Ma, a vent breccia complex, and a number of dikes. The largest of the satellite centers is the Flat Top center located southwest of the Akutan caldera and dated at 0.25 Ma. It consists of relatively

¹U.S. Geological Survey, Anchorage, Alaska

²University of Alaska, Fairbanks, Alaska

extensive flows, a vent breccia complex, and a radial dike swarm. The oldest of the satellite centers is the Long Valley series of linear and monolithologic domes or very shallow intrusions and carapace(?) breccias dated at 0.58 Ma. In addition, three remnant cinder cones overlie ancestral Akutan lavas north and west of the modern cone.

Most rocks of modern Akutan and its satellitic centers exhibit chemical characteristics of the tholeiitic magma series (fig. 3A) and, in large part, range from basalt to andesite in composition (50.3-62.9% SiO₂) (fig. 3B). Lava flows and pyroclastic deposits from the summit eruptions contain orthopyroxene, whereas lava flows from the satellite centers are typically orthopyroxene poor. Ancestral Akutan lava flows, on the other hand, tend to be more mafic (basalt and basaltic andesite) and contain as much as 8% phenocrystic olivine. The most silicic rock from the general Akutan center is a trachyte dike (67.8% SiO₂) that is probably related to a late satellitic cinder cone. Both the older subaerial and subaqueous volcanic rocks from the eastern part of the island are largely olivine-bearing basalts and basaltic andesites (48.5-53.3% SiO₂) (fig. 3B), similar in many respects to the lava flows from ancestral Akutan. In sharp contrast to these mafic rocks is a subaqueous silicic pyroclastic flow deposit exposed along the south shore of the island that contains clasts of rhyolitic obsidian (72.5% SiO₂). The source of this silicic deposit is offshore from Akutan island, possibly as far distant as Rootok Island, 12 km to the southeast.

Active fumaroles are presently confined to the summit intracaldera cone of modern Akutan (fig. 2) and to an area about 3 km east of the summit area in the upper reaches of Hot Springs Valley. Small hot springs issue from fluvial and beach deposits along the lower 1.5 km of Hot Springs Valley where they mix with the cold stream water and the water of Hot Springs Bay (Motyka and others, 1988)

The island exhibits a WNW structural grain as indicated by the orientation of recent ground cracks, faults, and to some extent, dikes. The recent ground cracks form a linear zone, 3 km long by 250 m wide and trending about N 60° W, that cuts across unconsolidated tephra and colluvium on the northwest side of the modern Akutan cone. These cracks apparently formed in response to a severe seismic swarm that occurred beneath the volcano in March 1996 (Power and others, 1997). Similarly, recent movement on two normal faults in older volcanic rocks in the eastern half of the island is also attributed to the 1996 seismic swarm. Most of the dikes throughout the east end of the island roughly parallel the WNW fault orientation. However, dikes on the west side of the island exhibit more diverse orientations, suggesting, in part, a radial arrangement around the Akutan cone.

ACKNOWLEDGEMENTS

We would like to recognize the early work of Frank M. Byers, Jr. and T.F.W. Barth of the U.S. Geological Survey who, in 1948, prepared a reconnaissance geologic map of Akutan Island (unpublished data) and a detailed map of Akutan's summit area (Byers and Barth, 1953). Their studies, on foot and by power dory and without benefit of topographic maps, are remarkable in their detail and insight and have been invaluable to us in this present investigation.

We are grateful to the people of the city of Akutan for welcoming us into their community. Joe Bereskin, Sr., Mayor of Akutan, and Jacob Stepetin, former Village Corporation President, are due special thanks for their advice and assistance with local logistics. Thanks also to Bret Joines, Superintendent of the Akutan Trident Seafoods processing plant, and Dave Abbasian, Assistant Superintendent, for their hospitality and logistical support. The Aleutians East Borough School District made

available to us a teacher's apartment, from which we based our operations, and opened the school for our use. And finally we thank the dogs of Akutan for biting only one of us.

Special thanks to our helicopter pilot, Paul Walters, who safely transported us around the island often during less than optimal conditions.

We are indebted to Jacqueline A. McIntire who painstakingly created the ARC/Info data base and plot for the geologic map, and to Linda L. Harris for the final preparation of the map. Thanks also to Kristi Wallace, Angie Roach, and Rusty Brown for their help in preparing the figures, and to Thomas P. Miller and Richard B. Moore for their careful reviews.

REFERENCES

- Byers, F.M., Jr. and Barth, T.F.W., 1953, Volcanic activity on Akun and Akutan Island: Proceedings Seventh Pacific Congress, Auckland and Christchurch, 1953, v.2, p. 382-197.
- Haq, B.U., Hardenbol, J., and Vail, P.R., 1987, The chronology of fluctuating sea levels since the Triassic: *Science*, v. 235, p. 1156-1167.
- LeBas, M.J., LeMaitre, R.W., Streckeisen, A., and Zanettin, B., 1986, A chemical classification of volcanic rocks based on the total alkali-silica diagram: *Journal of Petrology*, v. 27, p. 745-750.
- Miller, T.P., McGimsey, R.G., Richter, D.H., Riehle, J.R., Nye, C.J., Yount, M.E., and Dumoulin, J.A., 1998, Historically active volcanoes of Alaska: U.S. Geological Survey Open-File Report [in press].
- Miyashiro, Akiho, 1974, Volcanic rock series in island arcs and active continental margins: *American Journal of Science*, v. 274, p. 321-355.
- Motyka, R.J., Wescott, E.M., Turner, D.L., Swanson, S.E., Allely, R.D., and Larsen, Mark, 1988, Introduction and summary of geothermal investigations in Hot Springs Bay Valley, Akutan Island, Alaska in Motyka, R.J. and Nye, C.J., eds., A geological, geochemical, and geophysical survey of the geothermal resources at Hot Springs Bay Valley, Akutan Island, Alaska: Alaska Division of Geological and Geophysical Surveys, Report of Investigations 88-3, p. 1-10.
- Power, J.A., Paskievitch, J.A., Richter, D.H., McGimsey, R.G., Stelling, P., Jolly, A.D., and Fletcher, H.J., 1996, 1996 seismicity and ground deformation at Akutan Volcano, Alaska: *Eos, Transactions, American Geophysical Union*, v. 77, No. 46, p. F514.
- Romick, J.D., 1991, The igneous petrology and geochemistry of northern Akutan Island, Alaska: Alaska Division of Geological and Geophysical Surveys, Report of Investigations 90-3, 53 p.
- Romick, J.D., Perfit, M.R., Swanson, S.E., and Shuster, R.D., 1990, Magmatism in the eastern Aleutian Arc—Temporal characteristic of igneous activity on Akutan Island: *Contributions to Mineralogy and Petrology*, v. 104, p. 700-721.
- Stuiver, M. and Reimer, P.J., 1993, Extended ^{14}C data base and revised CALIB 3.0 ^{14}C age calibration program: *Radiocarbon*, v. 35, p. 215-230.
- Swanson, S.E. and Romick, J.D., 1988, Geology of northern Akutan Island, in Motyka, R.J. and Nye, C.J., eds., A geological, geochemical, and geophysical survey of the geothermal resources at Hot Springs Valley, Akutan Island, Alaska: Alaska Division of Geological and Geophysical Surveys Report of Investigations 88-3, p. 11-27.

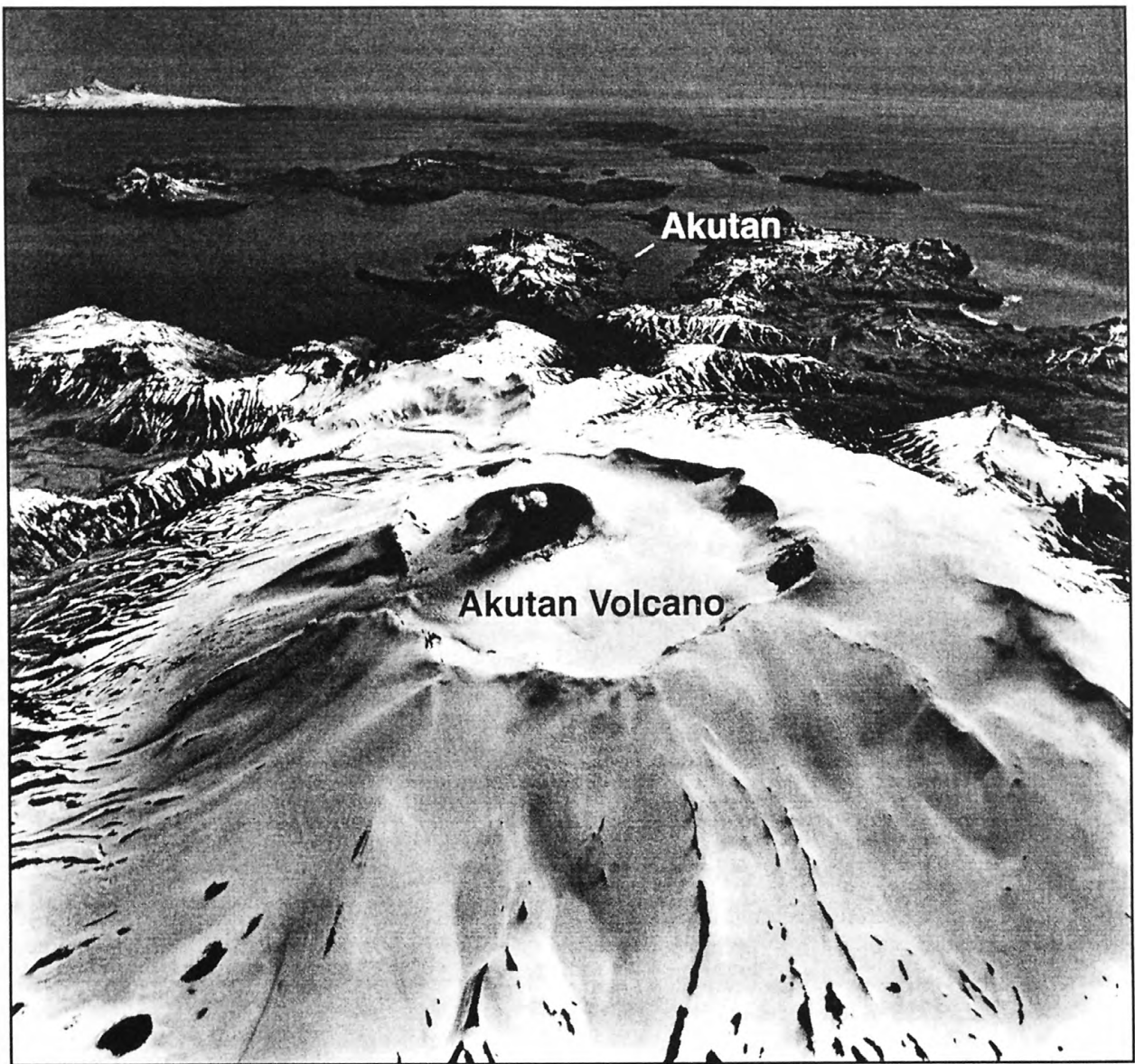


Figure 1. Oblique aerial view of Akutan Volcano and eastern part of Akutan Island from the west. Photo taken on June 7, 1983, showing unusually heavy snow cover and recent ash shower from intracaldera cone. Unimak Island is visible on far left horizon.

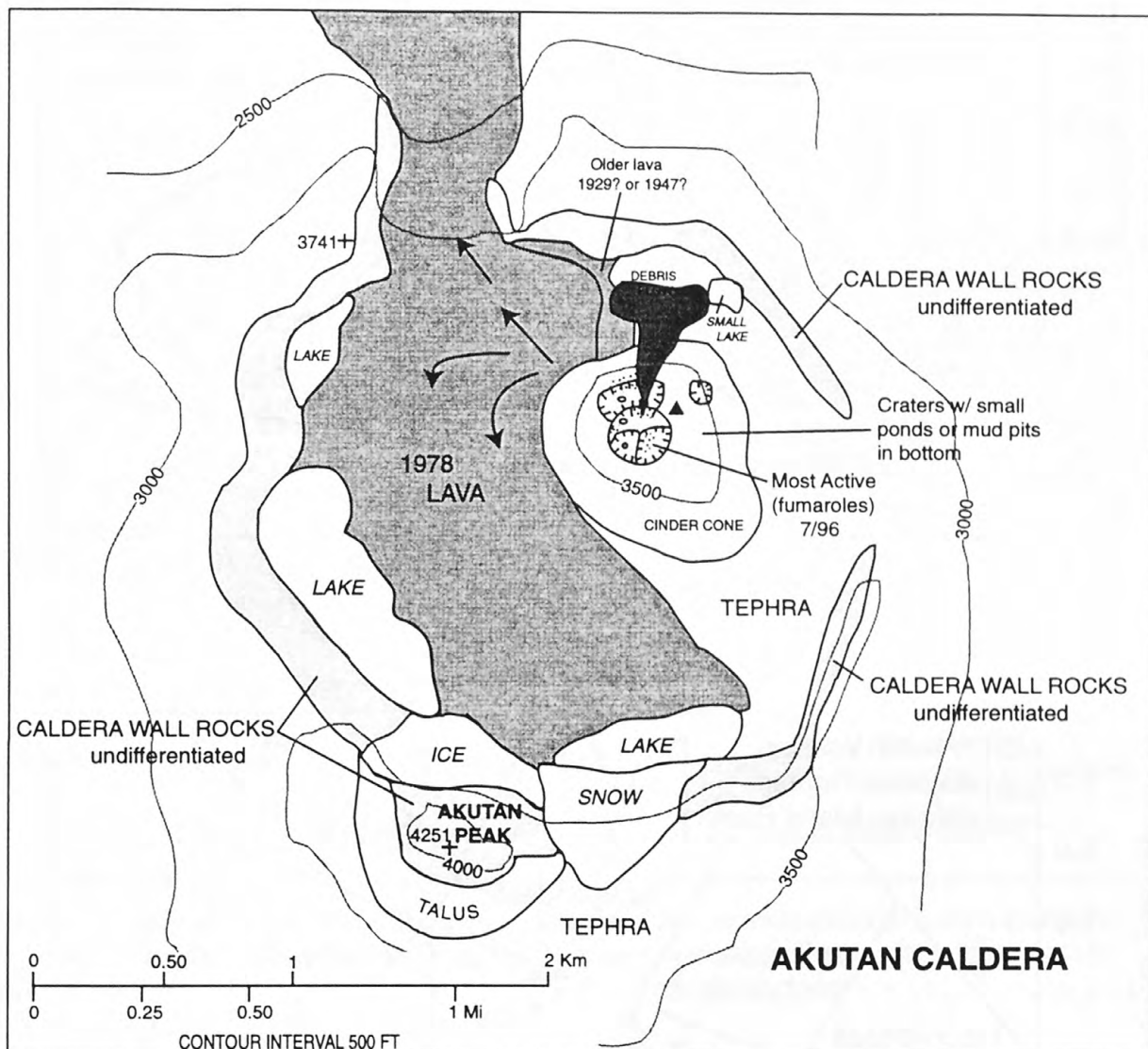


Figure 2. Detailed sketch map of Akutan caldera as of July 1996. Fumarole areas on intracaldera cone are shown by fine stipples.

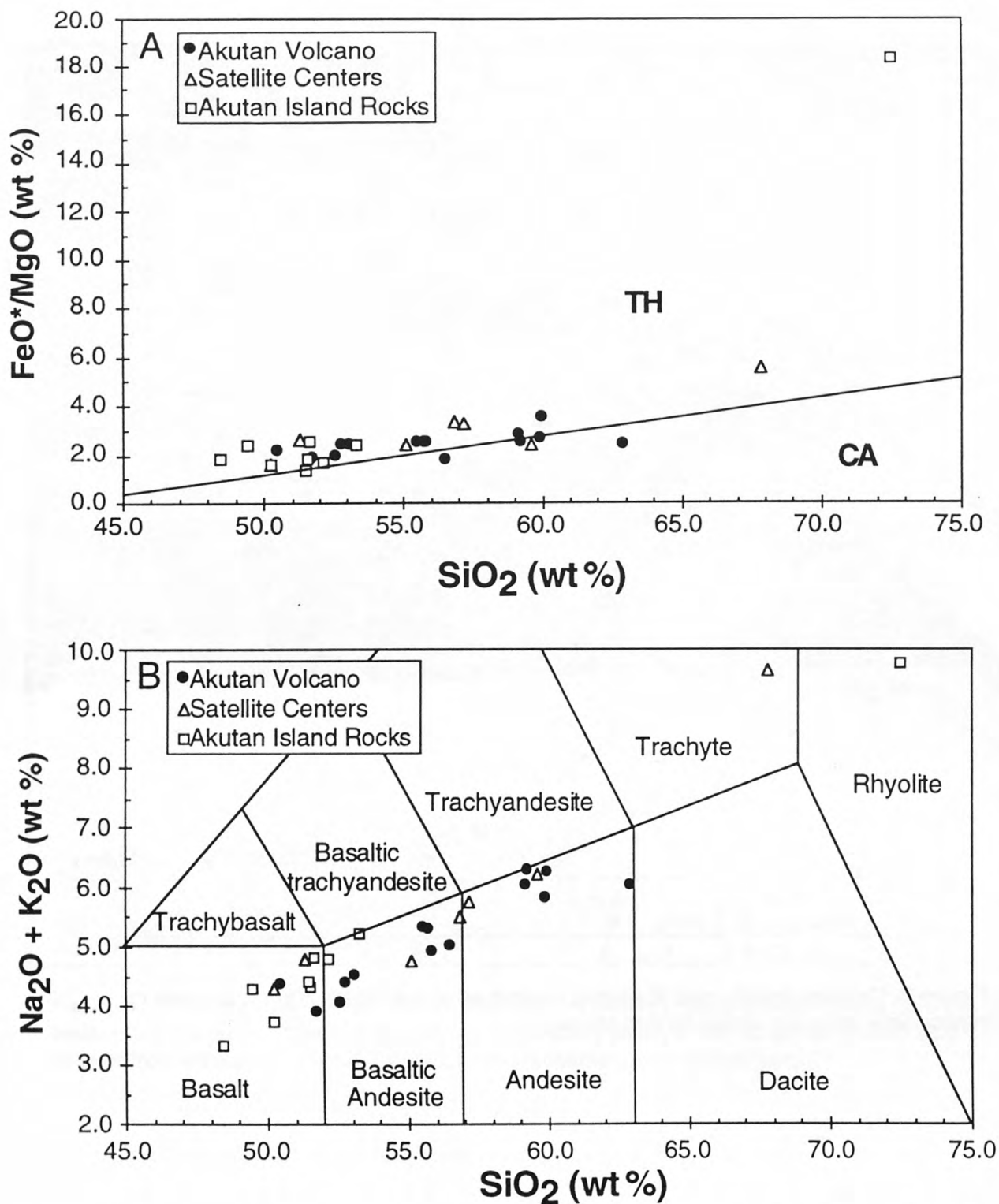


Figure 3. Variation diagrams for volcanic rocks from Akutan Island. Complete major and minor element chemistry is given in table 1 and sample locations are shown on the geologic map. (A) FeO*/MgO–silica diagram. Tholeiite–calcalkaline discriminant line from Miyashiro (1974). (B) Total alkali–silica diagram. Discriminant lines from LeBas and others (1986).

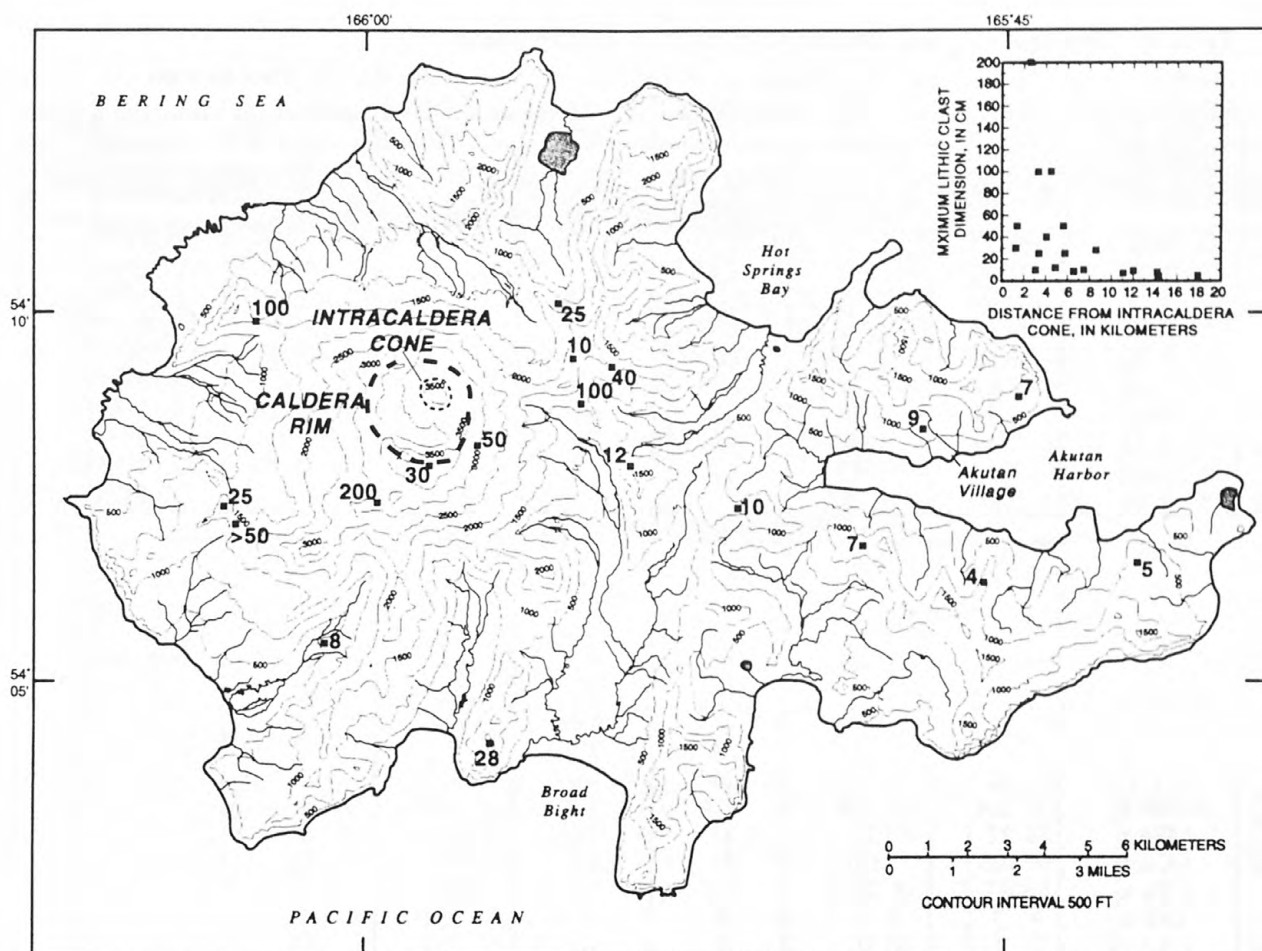


Figure 4. Map of Akutan Island showing location and size of lithic volcanic bombs probably ejected during the caldera-forming eruption. Numbers refer to maximum clast dimension, in centimeters.

Table 1. Chemical analyses of volcanic rocks from Akutan Island

[Analyses conducted at the GeoAnalytical Laboratory at Washington State University. Methods: Trace elements denoted with 'x' and major oxides by XRF. Trace elements denoted with 'i' by ICP-MS.]

Map Unit	1978	1929	1929?	Hsy	Hso	Qtu	
Locality No.	1	2	2	3	4	5	6
Sample No.	96-ARh-21	96-Mc-15C	96-Mc-15B	96-ARh-47	96-ARh-26	96-ARh-14A	96-Mc-31A
Normalized major-oxide composition in weight percent							
SiO ₂	55.73	55.49	55.82	52.58	59.15	52.77	53.07
Al ₂ O ₃	17.22	17.35	17.66	18.45	17.21	17.82	17.83
TiO ₂	1.164	1.122	0.930	1.030	0.896	1.239	1.231
FeO*	8.89	8.99	9.00	9.19	7.34	10.15	9.98
MnO	0.223	0.213	0.208	0.198	0.197	0.219	0.214
CaO	7.69	7.71	7.66	9.70	6.35	9.14	8.86
MgO	3.59	3.58	3.62	4.65	2.60	4.12	4.15
K ₂ O	0.89	0.89	0.84	0.66	1.19	0.59	0.62
Na ₂ O	4.40	4.45	4.08	3.39	4.85	3.81	3.91
P ₂ O ₅	0.211	0.203	0.176	0.146	0.223	0.137	0.140
Minor and trace element composition in ppm							
Ni x	0	0	0	5	2	0	0
Cr x	7	11	8	29	10	14	12
Sc x	27	26	25	35	21	26	30
V x	230	229	194	263	131	298	289
Ba x	329	334	322	262	409	242	237
Rb x	18	19	16	13	27	12	12
Sr x	361	367	387	390	334	410	407
Zr x	97	96	95	79	123	72	73
Y x	32	31	26	24	35	24	24
Nb x	2.4	1.9	1.8	1.2	2.8	1.7	1.1
Ga x	17	22	22	18	21	16	19
Cu x	105	101	69	101	67	70	114
Zn x	87	78	76	70	85	68	66
Pb x	7	9	8	6	15	2	7
La x	1	10	9	10	15	13	12
Ce x	10	21	28	12	18	9	4
Th x	5	3	4	5	4	4	1
La i	8.01	8.12	7.31	5.63	10.02	5.12	5.55
Ce i	18.27	18.56	16.80	12.85	22.78	11.63	12.64
Pr i	2.59	2.65	2.36	1.94	3.21	1.74	1.85
Nd i	12.94	13.02	11.60	9.42	15.59	8.91	9.42
Sm i	4.43	4.39	3.80	3.04	5.10	3.12	3.31
Eu i	1.44	1.40	1.29	1.06	1.50	1.20	1.23
Gd i	5.13	5.19	4.39	3.68	5.81	3.82	4.02
Tb i	0.91	0.90	0.76	0.66	1.02	0.71	0.70
Dy i	5.96	5.92	5.02	4.35	6.77	4.57	4.65
Ho i	1.26	1.26	1.06	0.91	1.42	0.97	1.00
Er i	3.54	3.57	2.98	2.57	4.02	2.79	2.82
Tm i	0.51	0.52	0.43	0.39	0.59	0.40	0.40
Yb i	3.24	3.32	2.75	2.41	3.69	2.50	2.53
Lu i	0.51	0.51	0.44	0.38	0.59	0.39	0.39
Ba i	310	316	321	231	395	222	229
Th i	1.46	1.50	1.48	1.18	2.12	0.89	0.99
Nb i	1.70	1.75	1.60	1.27	2.18	1.10	1.23
Y i	32.58	33.52	27.68	25.75	37.73	26.05	26.01
Hf i	2.73	2.82	2.68	2.02	3.66	1.87	1.96
Ta i	0.13	0.13	0.13	0.09	0.17	0.08	0.10
U i	0.84	0.90	0.85	0.61	1.24	0.52	0.57
Pb i	8.88	8.81	6.44	6.83	16.31	6.82	6.29
Rb i	19.2	20.0	17.3	14.4	25.8	12.5	13.7
Cs i	1.87	1.95	0.74	1.38	0.84	1.20	1.25
Sr i	369	368	389	402	333	427	417
Sc i	30.6	30.9	24.8	34.6	24.6	35.2	33.5

Map Unit	Qcw	Qocp	Qocd		Qol		Qaa	Hly
Locality No.	7	8	9	9	10	11	12	13
Sample No.	96-Mc-35	96-Mc-34	96-ARh-59L	96-ARh-59D	96-Mc-6	96-Mc-32B	96-ARh-38C	96-Mc-37C
Normalized major-oxide composition in weight percent								
SiO ₂	59.94	51.72	62.86	59.21	56.50	59.86	50.46	56.84
Al ₂ O ₃	16.58	18.39	16.96	17.62	16.77	17.51	19.03	18.24
TiO ₂	1.008	1.002	0.654	1.041	0.822	0.798	1.205	1.065
FeO*	7.87	9.53	5.82	6.64	7.90	6.83	10.31	8.14
MnO	0.218	0.199	0.121	0.185	0.168	0.172	0.202	0.204
CaO	5.64	10.10	5.01	6.08	8.28	6.17	9.42	7.35
MgO	2.23	5.03	2.38	2.67	4.34	2.55	4.74	2.48
K ₂ O	1.29	0.59	1.79	1.53	1.27	1.32	0.85	0.94
Na ₂ O	4.98	3.29	4.27	4.77	3.77	4.50	3.51	4.54
P ₂ O ₅	0.245	0.139	0.137	0.263	0.179	0.289	0.278	0.197
Minor and trace element composition in ppm								
Ni x	0	7	6	0	8	1	0	0
Cr x	4	29	9	5	49	8	15	8
Sc x	16	33	12	20	29	16	26	20
V x	95	282	121	129	195	112	290	143
Ba x	466	227	533	516	390	464	470	332
Rb x	30	12	39	30	26	23	13	20
Sr x	337	394	289	351	386	408	521	411
Zr x	133	73	170	153	133	151	123	101
Y x	38	22	32	37	28	36	24	32
Nb x	2.3	2.8	3.2	2.7	3.1	3.0	3.3	0.9
Ga x	20	24	20	20	19	19	25	18
Cu x	41	121	60	17	79	43	38	44
Zn x	85	71	69	81	75	76	89	71
Pb x	11	2	8	8	11	6	4	9
La x	23	1	14	11	11	10	7	14
Ce x	14	14	23	34	28	32	14	32
Th x	1	0	5	3	1	2	4	2
La i	10.24	5.37	10.64	13.48	10.60	11.61	12.92	7.59
Ce i	23.21	11.98	22.09	30.04	23.02	26.96	27.73	17.50
Pr i	3.28	1.78	3.03	4.09	3.15	3.82	3.88	2.51
Nd i	16.24	8.64	14.16	19.15	14.81	18.57	18.33	12.59
Sm i	5.28	3.09	4.18	5.76	4.46	5.59	5.13	4.15
Eu i	1.60	1.07	1.21	1.64	1.24	1.59	1.57	1.39
Gd i	6.14	3.65	4.60	6.39	4.71	6.05	4.91	5.04
Tb i	1.07	0.65	0.82	1.09	0.79	1.04	0.81	0.88
Dy i	6.98	4.19	5.33	7.01	5.15	6.45	5.00	5.63
Ho i	1.53	0.90	1.18	1.50	1.08	1.40	1.02	1.22
Er i	4.35	2.52	3.40	4.15	3.02	3.97	2.84	3.45
Tm i	0.63	0.37	0.51	0.61	0.44	0.58	0.40	0.51
Yb i	4.02	2.30	3.31	3.90	2.86	3.80	2.45	3.25
Lu i	0.64	0.37	0.53	0.61	0.46	0.61	0.38	0.50
Ba i	420	213	508	501	380	433	449	320
Th i	2.35	0.88	3.49	3.44	2.46	2.34	1.95	1.44
Nb i	2.42	1.08	3.38	3.41	2.59	3.19	3.41	1.63
Y i	41.78	23.99	33.77	39.57	29.37	39.33	26.29	32.89
Hf i	4.04	1.87	5.02	4.49	3.73	4.42	3.19	2.71
Ta i	0.20	0.09	0.26	0.25	0.20	0.25	0.24	0.13
U i	1.39	0.56	1.92	1.88	1.40	1.32	0.87	0.84
Pb i	10.70	0.46	9.16	10.05	10.06	6.40	3.71	9.76
Rb i	31.1	13.5	39.6	30.3	26.1	24.3	14.1	20.2
Cs i	3.07	0.82	1.06	1.53	0.96	0.53	0.84	2.02
Sr i	346	400	287	360	392	418	524	404
Sc i	24.7	37.2	16.1	25.0	30.0	18.5	24.7	24.6

Map Unit	Hlo	Qld	Qfl		Qcl	Qccd	QTg
Locality No.	14	15	16	17	18	19	20
Sample No.	96-Mc-37B	96-ARh-56	96-ARh-24A	96-Mc-31B	96-ARh-53D	96-ARh-38D	96-ARh-10
Normalized major-oxide composition in weight percent							
SiO ₂	57.19	59.59	51.33	50.25	55.10	67.83	51.68
Al ₂ O ₃	18.25	17.38	20.78	18.53	18.81	16.25	19.69
TiO ₂	1.049	0.805	1.121	1.060	0.959	0.578	1.187
FeO*	7.73	6.58	8.76	9.45	8.34	3.15	9.31
MnO	0.200	0.239	0.179	0.177	0.186	0.169	0.193
CaO	7.26	6.22	9.45	10.16	8.25	1.68	9.14
MgO	2.38	2.80	3.41	5.91	3.49	0.57	3.71
K ₂ O	0.95	1.75	0.84	1.22	0.98	3.01	1.14
Na ₂ O	4.79	4.44	3.93	3.04	3.75	6.63	3.65
P ₂ O ₅	0.202	0.195	0.195	0.198	0.145	0.131	0.302
Minor and trace element composition in ppm							
Ni x	0	5	0	20	0	6	6
Cr x	7	23	10	50	12	0	28
Sc x	22	19	28	32	27	5	20
V x	134	145	244	329	238	22	232
Ba x	344	478	306	361	340	1139	556
Rb x	21	38	12	17	20	65	25
Sr x	409	341	430	615	391	248	667
Zr x	101	158	97	103	101	234	114
Y x	31	32	26	21	25	46	23
Nb x	1.1	3.8	2.5	1.7	2.4	8.1	3.1
Ga x	17	19	23	21	17	20	19
Cu x	47	37	83	†156	64	2	52
Zn x	73	72	77	85	69	86	78
Pb x	11	8	3	2	6	8	6
La x	11	18	6	20	11	23	36
Ce x	22	28	2	40	38	69	35
Th x	0	3	3	3	3	8	4
La i	7.94	12.32	8.17	9.27	8.14	24.17	14.58
Ce i	18.12	26.93	18.44	19.35	17.95	55.17	30.71
Pr i	2.63	3.57	2.61	2.66	2.37	7.14	4.16
Nd i	13.20	16.59	12.67	12.47	11.33	31.87	19.31
Sm i	4.28	4.88	4.10	3.45	3.56	8.50	5.27
Eu i	1.44	1.39	1.34	1.11	1.13	2.06	1.67
Gd i	5.26	5.18	4.61	3.62	4.02	8.22	4.86
Tb i	0.93	0.88	0.77	0.62	0.69	1.40	0.77
Dy i	5.97	5.67	4.97	3.88	4.53	8.50	4.63
Ho i	1.27	1.21	1.04	0.81	0.95	1.79	0.92
Er i	3.57	3.42	2.85	2.20	2.75	5.06	2.48
Tm i	0.52	0.50	0.42	0.32	0.39	0.75	0.35
Yb i	3.36	3.22	2.58	1.97	2.56	4.85	2.21
Lu i	0.53	0.51	0.41	0.31	0.40	0.76	0.35
Ba i	319	464	293	340	314	1130	542
Th i	1.60	3.58	1.30	2.07	2.19	6.07	2.14
Nb i	1.71	3.20	2.04	1.96	2.02	7.76	3.25
Y i	34.99	33.66	27.29	21.80	25.61	48.75	24.20
Hf i	2.86	4.39	2.58	2.44	2.75	6.88	2.66
Ta i	0.15	0.25	0.14	0.13	0.15	0.54	0.22
U i	0.99	1.87	0.68	1.13	1.15	2.97	1.05
Pb i	9.36	6.34	4.83	6.80	6.42	7.87	4.23
Rb i	21.2	35.6	12.1	17.7	18.8	61.8	24.2
Cs i	2.13	0.86	0.67	0.76	0.65	1.27	2.09
Sr i	418	358	429	619	380	245	660
Sc i	25.8	21.6	27.5	36.1	27.6	11.7	19.0

Map Unit	QTd			QTV				
Locality No.	21	22	23	24	25	26	27	28
Sample No.	96-ARh-2	96-ARh-7	96-Mc-5	96-ARh-1	96-ARh-5	96-ARh-6	96-ARh-12A	96-Mc-28
Normalized major-oxide composition in weight percent								
SiO ₂	51.55	51.50	50.28	49.46	53.29	52.16	48.48	72.49
Al ₂ O ₃	17.70	17.12	18.47	18.69	17.47	18.58	18.84	13.76
TiO ₂	1.071	1.000	0.940	1.427	1.326	1.063	1.197	0.235
FeO*	9.37	8.86	8.95	10.59	9.46	8.14	10.35	2.60
MnO	0.178	0.174	0.164	0.197	0.196	0.160	0.179	0.080
CaO	10.24	10.15	11.58	10.53	8.61	9.89	11.79	0.90
MgO	5.28	6.51	5.75	4.57	3.96	4.99	5.69	0.14
K ₂ O	1.21	1.19	0.89	1.18	1.46	1.34	0.72	4.92
Na ₂ O	3.11	3.19	2.82	3.10	3.73	3.42	2.60	4.83
P ₂ O ₅	0.301	0.291	0.161	0.264	0.498	0.253	0.160	0.035
Minor and trace element composition in ppm								
Ni x	17	52	23	9	5	15	12	8
Cr x	77	174	72	35	22	37	52	0
Sc x	29	32	34	31	26	31	39	3
V x	249	236	272	402	196	253	374	3
Ba x	480	457	283	495	446	310	277	1043
Rb x	24	24	18	21	29	18	11	119
Sr x	520	517	448	490	422	566	479	48
Zr x	134	129	94	109	205	141	74	407
Y x	26	23	21	25	42	22	19	†59
Nb x	4.6	4.5	1.8	3.2	7.8	6.7	2.8	14.9
Ga x	19	19	18	22	22	19	23	17
Cu x	77	75	125	†174	103	40	124	24
Zn x	78	76	69	94	87	70	73	62
Pb x	3	6	7	2	5	5	0	19
La x	26	8	11	18	21	30	21	42
Ce x	28	26	11	22	43	29	19	82
Th x	4	5	2	7	5	2	2	10
La i	14.33	14.46	7.79	12.64	17.94	14.67	7.82	33.51
Ce i	30.71	30.90	17.09	26.87	40.84	31.47	16.87	70.64
Pr i	4.26	4.20	2.36	3.80	5.95	4.17	2.47	8.77
Nd i	19.51	19.05	11.26	17.93	28.78	18.81	11.94	36.34
Sm i	5.13	5.19	3.42	5.05	8.01	5.18	3.41	9.52
Eu i	1.45	1.48	1.05	1.56	2.05	1.54	1.21	0.99
Gd i	5.13	4.94	3.70	4.93	8.17	4.73	3.59	8.88
Tb i	0.82	0.78	0.63	0.81	1.31	0.76	0.58	1.58
Dy i	4.94	4.82	4.02	4.92	8.25	4.40	3.72	10.05
Ho i	1.01	0.97	0.86	1.00	1.66	0.89	0.77	2.14
Er i	2.82	2.62	2.36	2.70	4.59	2.35	2.11	6.21
Tm i	0.40	0.38	0.33	0.38	0.67	0.33	0.29	0.95
Yb i	2.51	2.38	2.12	2.39	4.07	2.05	1.82	6.25
Lu i	0.40	0.36	0.33	0.36	0.65	0.32	0.28	0.98
Ba i	446	442	260	463	420	299	256	1024
Th i	2.84	2.83	1.98	2.33	2.58	1.91	1.12	11.75
Nb i	4.09	3.99	1.87	3.33	6.79	6.17	2.05	13.74
Y i	27.82	25.41	22.30	25.32	46.35	22.83	21.08	59.52
Hf i	3.46	3.42	2.49	2.81	5.69	3.67	1.69	12.40
Ta i	0.28	0.27	0.14	0.24	0.46	0.45	0.14	1.06
U i	1.40	1.42	1.07	1.08	1.30	0.92	0.51	5.78
Pb i	6.80	6.33	5.89	3.60	6.15	2.35	2.59	20.03
Rb i	24.8	23.5	17.7	23.5	28.3	18.3	13.9	116.7
Cs i	1.30	1.42	0.65	0.31	1.47	0.24	1.90	5.73
Sr i	542	527	452	516	439	575	503	51
Sc i	33.1	32.0	38.4	34.5	27.4	31.8	43.2	7.0

Table 2. Radiocarbon dates associated with tephra assumed to be product of Akutan caldera formation
 [All material dated was humic fraction, soil organic matter; dates calibrated using method of Stuiver and Reimer (1993);
 BP (before present) ages reported with respect to year AD 1950]

Sample No.	Location (Map. No.)	Lab No.	Reported Age (14C yr BP)	$\delta^{13}\text{C}_{\text{PDB}}$	Calibrated 2 σ Age Range (yr BP)	Calibrated age estimate (yr BP)
96CW59-1	Broad Bight (1)	GX-22618 (AMS)	1,940 \pm 60	-25.7	1998-1713	1881
96CW65-4	Hot Springs Valley (2)	GX-22620	1,530 \pm 85	-27.5	1592-1285	1408
96CW67-1	Hot Springs Bay Coast (3)	GX-22621	1,700 \pm 120	-25.8	1882-1313	1580
96CW81-2	Flat Bight (4)	GX-22624	1,520 \pm 80	-27.1	1559-1285	1406
96CW85-2	Long Valley (5)	GX-22626	1,775 \pm 90	-27.3	1917-1420	1660
96CW94-3	Akutan Harbor (6)	GX-22628	1,550 \pm 170	-25.9	1857-1086	1411
				Mean weighted ^{14}C age		1611

Table 3. $^{40}\text{Ar}/^{39}\text{Ar}$ ages of volcanic rocks from Akutan Island

[Analyses performed by P. Layer in the laboratories of the Geophysical Institute, University of Alaska Fairbanks]

Locality Letter	Sample No.	Map Unit	Number of Analyses	Mean Age ¹ (ma)	Isochron Age ¹ (ma)
A	96ARh-5	QTv	9 plus 1 step heat	--	Excess argon 3.29±0.11 $^{40}\text{Ar}/^{36}\text{Ar}_i=309\pm3$
B	96ARh-60A	QTv	9	2.34±0.07	Excess argon?? 1.46±0.51 $^{40}\text{Ar}/^{36}\text{Ar}_i=308\pm7$
C	96ARh-7	QTd	9	1.55±0.04	Excess argon?? 1.22±0.16 $^{40}\text{Ar}/^{36}\text{Ar}_i=310\pm7$
D	96ARh-38c	Qaa	4	1.41±0.04	No isochron
E	96ARh-56	Qld	6	0.58±0.03	Excess argon?? 0.36±0.14 $^{40}\text{Ar}/^{36}\text{Ar}_i=306\pm7$
F	96Mc-32B	Qol	8	0.36±0.05	Atmos argon 0.31±0.11 $^{40}\text{Ar}/^{36}\text{Ar}_i=297\pm3$
G	96ARh-24A	Qfl	6	0.25±0.04	No isochron
H	96ARh-53D	Qcl	4	0.15±0.05	Atmos argon 0.25±0.16 $^{40}\text{Ar}/^{36}\text{Ar}_i=288\pm12$
I	96ARh-59B	Qocu	6 plus 1 step heat	0.45±0.12	Excess argon 0.04±0.06 $^{40}\text{Ar}/^{36}\text{Ar}_i=305\pm1$

¹**Mean and isochron ages:** Weighted mean of a unimodal distribution of ages of the whole-rock analyses. For some samples, isochron analysis indicates excess argon. However, the regression in most cases is not significant. For samples 5 and 59B, step-heating clearly shows the excess argon; in these cases, the age quoted is an isochron age, calculated from single grains and step-heat fractions. Best estimate of the age of the samples is shown in **bold**.

DESCRIPTION OF MAP UNITS

Surficial Deposits (not related to Akutan Volcano)

Alluvial deposits (Holocene)

- Qa Alluvium in active stream channels and alluvial fans. Deposits range from well-sorted silt, sand, and gravel in stream channels to moderately to poorly sorted silt, sand, and gravel in alluvial fans. May include minor interbedded tephra.
- Qau Alluvium, undifferentiated. Includes thick deposits (>2 m) of silt, sand, and gravel in terraces along active stream channels; thin deposits (<2 m) of silt, sand, and gravel in extensive flood plains; and silt, sand, and gravel in small alluvial fans bordering the flood plains. May include minor tephra and thin lahar runout deposits.

Colluvial deposits (Holocene)

- Qcu Colluvium, undifferentiated. Chiefly talus, small landslides, lobate deposits of small debris flows, and other deposits of mass-wasting processes, and minor alluvium in small fans and cones generally at the base of steep hillslopes. Deposits may include a large proportion of primary and reworked tephra and are locally gradational with the tephra deposits of map unit Qtu. Deposits consist chiefly of poorly sorted silt, sand, gravel, and boulders, but include angular blocks, boulders, and gravel in rock-fall talus and landslides. In the vicinity of the active fumaroles at the head of Hot Springs Bay, colluvium contains abundant well-rounded boulders, as much as 1 m in diameter, suggestive of glacial origin. Alternatively, these boulders may have been derived from subjacent volcanoclastic deposits.

Lacustrine deposits (Holocene)

- Ql Lake and bog-marsh deposits. Includes well-sorted silt and sand along margins of present day lakes or drained lake basins and silt and minor clay and sand in bog-marsh deposits. Bog-marsh deposits may contain standing water and variable amounts of peat.

Eolian deposits (Holocene)

- Qse Dune sand. Thick (>2 m) accumulations of well-sorted fine-to-medium sand in linear dunes. Found at the mouths of some broad valleys near modern beaches along north shore of island. May include minor amounts of beach sand, alluvium, and tephra.

Beach deposits (Holocene)

- Qb Modern beaches. Well-sorted sand, gravel, and boulders along present shoreline. Deposits range from entirely sand to entirely well-rounded boulders. May include minor amounts of tephra, alluvium, eolian sand, and colluvium.
- Qba Abandoned beaches. Well-sorted sand, gravel, and boulders along present shoreline, landward of modern beaches. Deposits range from entirely sand to entirely well-rounded boulders. May include minor amounts of alluvium, eolian sand, and colluvium. Usually forms nested sets of parallel ridges marking the position of former coastlines.

Deposits of Akutan and Ancestral Akutan Volcano

Historic lava flows and cinder cone (Holocene)

- 1978 Eruption of 1978. Lava flows filled much of the present caldera, escaped through a breach in the caldera wall, and flowed down the north flank of volcano. Intracaldera lava flows covered most of the lava flows from the 1947-48 eruption that was confined to the caldera. Flows outside the caldera are as much as 8 m thick and exhibit blocky rubble carapaces and well-developed flow levees. The 1978 lava is a dark gray, porphyritic basaltic andesite (55.7% SiO₂, loc. 1, table 1) containing phenocrysts of plagioclase (10-20%, 3 mm), clinopyroxene (2-5%, 2 mm), and orthopyroxene (1-3%, 1 mm) in a cryptocrystalline groundmass.
- 1929 Eruption of 1929. Lava flows are exposed in two kipukas within the 1978 lava flows on the north flank of the volcano. In a narrow ravine in one kipuka, lava flows overlie an older flow that may represent a pre-1929 flow or an early phase of the 1929 flow as both flows are mineralogically and chemically similar. The lavas are dark gray to medium dark gray porphyritic basaltic andesite containing phenocrysts of plagioclase (12-20%, 3 mm), clinopyroxene (2-5%, 3 mm), and orthopyroxene (2-4%, 2 mm) in a cryptocrystalline groundmass. Samples contain 55.5% SiO₂ (1929 flow) and 55.8% SiO₂ (1929(?) flow (loc. 2, table 1).
- Hc Modern cinder cone. Marks site of only known intracaldera vent and is source of all historic eruptions and older Holocene activity. Cone is composed chiefly of cinder, bombs, finer grained pyroclastic debris, agglutinates, small

pyroclastic flows, and hot and cold debris avalanches from largely Strombolian activity. Active fumaroles are present on the summit area (see fig. 2 for details of intracaldera geology).

Holocene lavas (Holocene)--Young lava flows, other than those from the Lava Point satellitic center, are recognized in three areas on the flanks of Akutan Volcano: in the Sea Lion Rocks area south of Lava Point and high in the drainages of Cascade and Broad Bights. The lava flows exposed in Cascade and Broad Bights are clinopyroxene-orthopyroxene-olivine andesites, typical of the flows erupted from the summit area, whereas the Sea Lion Rocks flows are clinopyroxene-olivine andesites suggesting a satellitic source.

- Hsy Younger Sea Lion Rocks lava flow. Single(?) flow largely covered by tephra. Rock is a medium dark gray highly porphyritic andesite (52.6% SiO₂, loc. 3, table 1) containing phenocrysts of plagioclase (15-25%, 4 mm), clinopyroxene (4-8%, 3 mm), and olivine (1%, 1 mm) in a pilotaxitic groundmass.
- Hso Older Sea Lion Rocks lava flow. Thick (about 30 m), single(?) flow commonly exhibiting massive columnar joints in well-formed colonnades. Rock is an andesite (59.2% SiO₂, loc. 4, table 1) physically similar to Hsy, but less porphyritic containing phenocrysts of plagioclase (4-8%, 2 mm) and clinopyroxene (1-4%, 1 mm) in a pilotaxitic groundmass. Top of colonnades, where present about 1 m above mean sea level, provide habitat for Steller sea lions.
- Hf Holocene lava flows. The distal ends of two, thick (>20 m) flows are exposed on the south and southeast flanks of the volcano. The upper ends of the flows are covered by younger tephra deposits

(unit Qtu). The rocks of both flows are similar. They are dark gray to medium dark gray porphyritic andesites containing phenocrysts of plagioclase (8-15%, 3-4 mm), clinopyroxene (2-6%, 2-4 mm), orthopyroxene (trace-2%, 1 mm), and olivine (0-2%) in a glassy to cryptocrystalline groundmass. These flows are mineralogically similar to the dense, lithic bombs (52.8-53.1% SiO₂, loc. 5 and 6, table 1) that are found on the surface over the entire island (fig. 4) and a widespread black, scoriaceous tephra (see description in unit Qtu) dated at 1611 years B.P. (table 2). The flows are interpreted to have erupted during formation of the present caldera.

Volcaniclastic deposits (Holocene and Pleistocene)

Qv Volcaniclastic deposits, undifferentiated. Chiefly lahars but includes minor pyroclastic-flow deposits in Long Valley and Reef Bight and interbedded tephra. Lahars fill most of the valleys that head on the flanks of Akutan Volcano and consist of thick accumulations (40 to 60 m total thickness in Long Valley) of boulders, gravel, sand, and silt. The deposits are poorly sorted, clast- and matrix-supported, locally well indurated, hard, and compact. Some deposits contain juvenile magmatic material indicating that some lahars may have formed from pyroclastic flows higher on the flanks of the volcano. The pyroclastic-flow deposits consist largely of stratified, matrix supported gravel including abundant juvenile magmatic clasts; vertical gas-escape structures are locally common. Thin interbedded tephra deposits locally separate individual lahars, especially in the valleys of Broad, Cascade, and Reef Bights. A black, scoriaceous tephra, as much as 2 m thick, that occurs near the base of

the lahars in Long Valley and Broad Bight and is also present in tephra sections (unit Qtu) elsewhere on the island has been radiocarbon dated at 1611 years B.P. (table 2). Juvenile clasts in the black scoriaceous tephra are mineralogically similar to the widespread lithic bombs (fig. 4) present on all upland surfaces throughout the island and the young, post-glacial lava flows (unit Hf) on the south and southeast slopes of the modern Akutan cone, suggesting that the black tephra, lithic bombs, lava flows, and the lahars of Long Valley and probably Broad Bight were the products of a major Strombolian or sub-Plinian eruption that was responsible for the formation of the present caldera.

Qlr Lahar runout deposits. Distal equivalents of lahar deposits (in unit Qv) representing the downstream flow transformation from lahar to sediment-laden (hyperconcentrated) streamflow. Chiefly sand, silt, and minor gravel in 1- to 4-m-thick accumulations in Broad Bight valley.

Qdf Reworked lahars. Chiefly poorly sorted, bouldery gravel formed by reworking of primary lahar deposits. May be both matrix and clast supported. Observed only in the valley bottom of Cascade Bight and in the upper west fork of Broad Bight valley.

Qtu Tephra. Includes young Holocene tephra on the present Akutan Volcano cone and undifferentiated tephra beyond the present cone.

Young tephra consists of ash- to block-sized pyroclasts in accumulations locally exceeding 10 m. Thickness and pyroclast size generally increase toward the summit of the volcano. One of the youngest tephra beds is a black, scoria-

ceous unit, up to 2 m thick, that occurs interbedded with lahars in unit Qv and is widespread elsewhere on the island in this (Qtu) map unit. Soil organic matter associated with this tephra has yielded an average calibrated age of 1611 years B.P. (table 2). Lithic bombs in the black, scoriaceous tephra unit are mineralogically similar to lithic bombs, as much as 2 m in diameter, of porphyritic clinopyroxene-orthopyroxene basaltic andesite (52.8- 53.1% SiO₂, loc. 5 and 6, table 1) that occur as lag deposits (?) on most upland surfaces throughout the island (fig. 4). As discussed previously in the description of the undifferentiated volcanoclastic deposits of unit Qv, this island-wide black tephra and the lithic bombs are believed to be eruptive products from the formation of the present caldera.

Tephra deposits, high on the southwest flank of the present cone, mantle, and are incorporated with, extensive boulder deposits that may represent deposits of Holocene glaciation.

Beyond the present cone of Akutan, the tephra deposits—in addition to the black, scoriaceous tephra—include other Holocene tephra from the present cone and older tephra from ancestral Akutan, the satellitic centers, and unknown sources off the island. These distal deposits consist chiefly of layered ash and lapilli in accumulations as much as 5 m thick, on most level and low-gradient slopes. Gradational with colluvium (Qcu) at the base of colluvium-covered slopes.

Present caldera wall rocks, undifferentiated (Holocene and Pleistocene)

Qcw Includes flows, agglutinates, and pyroclastic deposits exposed high on the rim of the present Akutan caldera. A sample of one flow is a grayish-black, porphy-

ritic andesite (59.9% SiO₂, loc. 7, table 1) containing phenocrysts of plagioclase (10-20%, 4 mm), clinopyroxene (1-5%, 3 mm), orthopyroxene (1-4%, 5 mm) and olivine (trace-1%) in a glassy groundmass.

Older caldera wall rocks (Pleistocene)—

Remnants of an older caldera are exposed on Akutan Volcano southwest of the present caldera. Akutan Peak, high point on the present caldera wall, may represent a major eruptive center in the old caldera.

Qocp Plug. Massive intrusive exposed on Akutan Peak in wall of present caldera. Rock, collected from talus at foot of peak, is a medium gray, porphyritic basalt (51.1% SiO₂, loc. 8, table 1) containing phenocrysts of plagioclase (15-30%, 4 mm), clinopyroxene (1-6%, 2 mm), and olivine (1-5%, 1 mm) in a cryptocrystalline groundmass.

Qocd Dome. Small dome or thick flow of banded, mixed magma, of porphyritic high-silica andesite. Light bands (62.8% SiO₂, loc. 9, table 1) are medium gray and consist of small phenocrysts of plagioclase (5-10%, 1 mm), and clinopyroxene (trace-2%, <1 mm) in a trachytic groundmass of plagioclase microlites; dark bands (59.2% SiO₂, loc. 9, table 1) are medium dark gray and consist of phenocrysts of plagioclase (5-10%, 2 mm), clinopyroxene (1-3%, 1.5 mm), and orthopyroxene (trace-1%, <1 mm) in a cryptofelsitic groundmass.

Qocu Volcanic rocks, undifferentiated. Chiefly lithic-rich agglutinates, lava flows, bedded lapilli tuffs, and bomb-rich pyroclastic flows. Agglutinates and flows are olive gray to medium dark gray porphyritic andesites containing phenocrysts of plagioclase (10-15%, 3-5 mm), clinopyroxene (1-6%, 2-3 mm),

and orthopyroxene (trace-2%, 1 mm) in a crypto-crystalline groundmass. A $^{40}\text{Ar}/^{39}\text{Ar}$ isochron age of 0.04 ± 0.06 Ma (loc. I, table 3) is not significant due to excess argon.

Qol Pre-glacial lavas (Pleistocene)—Lava flows are exposed locally, mostly around base of present Akutan cone; elsewhere covered by Holocene tephra (Qtu). Flows are typically thick (>5 m) and tend to form prominent cliffs. Rocks are medium gray, dark gray and olive gray porphyritic andesites (56.5-59.8% SiO_2 , loc. 10 and 11, table 1) containing phenocrysts of plagioclase (5-30%, 4-5 mm), clinopyroxene (1-7%, 3 mm), orthopyroxene (trace-4%, 1-5 mm), and olivine (0-1%, 2 mm) in cryptocrystalline to pilotaxitic groundmasses. Whole rock $^{40}\text{Ar}/^{39}\text{Ar}$ mean age of andesite (loc. F, table 3) is 0.36 ± 0.05 Ma.

Volcanic rocks of ancestral Akutan Volcano (Pleistocene)—Lava flows and minor subaerial lahars and airfall deposits that dip gently away from the present Akutan summit area. Rocks are mainly olivine-rich basalts and basaltic andesites. Subaerial lava flows and volcanoclastic deposits in the eastern part of the island, especially those nearest the present Akutan cone and shown as unit QTV on the geologic map, may also be products of ancestral Akutan Volcano.

Qaa Lava flows and minor volcanoclastic rocks, undifferentiated. Chiefly medium (3-4 m thick) to thick (>5 m) flows interlayered with minor lahars and airfall lapilli tuffs, especially at higher elevations. Flows are medium to dark gray and range from fine-grained aphanitic to highly porphyritic. Porphyritic varieties are basalts (50.5% SiO_2 , loc. 12, table 1) and basaltic andesites containing phenocrysts of plagioclase (10-40%, 1-5 mm), olivine (1-8%, 2-3 mm), and

clinopyroxene (0-20%, 2-3 mm) in intersertal to intergranular groundmasses. Whole rock $^{40}\text{Ar}/^{39}\text{Ar}$ mean age of basalt (loc. D, table 3) is 1.41 ± 0.04 Ma.

Qac Cinder cone. Local accumulations of palagonitized cinder and scoria interlayered with lava flows of unit Qaa.

Qap Plug. Linear plug or massive dike of basaltic andesite (?) extends out from cinder cone (Qac) south of Lava Point. Plug forms natural barrier to young Lava Point flows (Hlo).

Satellite Centers

Lava Point lava flows and cinder cone (Holocene)—Lava flows from a well-preserved cinder cone form a large lava pad of about 13 km^2 extending into the sea at the northwest end of the island. Age of the Lava Point eruptive activity is not known. There is some evidence of activity in the late 1920's, but much, if not all, of the lava flows were probably erupted prior to 1870. At least two distinct flow units (separated by dashed line on map) are recognized based on physical features and lichen and plant growth. The older unit (Hlo) consists of a series of near temporal flows that flowed to the west and southwest; the younger unit (Hly) is apparently a single flow that flowed to the north and northwest. All lavas are clinopyroxene-olivine andesites, chemically and mineralogically distinct from Akutan summit lavas.

Hly Younger lava flow. Massive flow, locally more than 20 m thick, with well-preserved blocky rubble surface. Rock is a medium dark gray, porphyritic andesite (56.8% SiO_2 , loc. 13, table 1) containing phenocrysts of plagioclase (10-15%, 3-4 mm), clinopyroxene (1-4%, 2 mm), and olivine (trace-1%, 1 mm) in a cryptocrystalline groundmass.

Hlo Older lava flows. Physically similar to younger flow (Hly) but consists of a number of flows that were erupted at about the same time. Rock is a dark gray, porphyritic andesite (57.2% SiO₂, loc. 14, table 1) containing phenocrysts of plagioclase (5-10%, 2 mm), clinopyroxene (1-4%, 2 mm), and olivine (trace) in a pilotaxitic groundmass.

Hlc Cinder cone. Well-preserved cone with small summit crater. Consists chiefly of cinder, bombs, and other pyroclastic debris.

Long Valley dome (?) complex

(Pleistocene)—Complex consists of a roughly linear chain of largely brecciated domes or shallow intrusives at the head of Long Valley, northeast of the present Akutan Volcano. Large areas of the complex have been affected by hydrothermal alteration.

Qlf Lava flow. Short, thick (>25 m), columnar-jointed flow, that appears to have been erupted from the center of the complex. Flow was not accessible for sampling.

Qld Domes. Massive, structureless bodies, as much as 1 km in diameter, enclosed in mineralogically similar monolithic breccias. Rock is dark gray to olive black, porphyritic andesite (59.6% SiO₂, loc. 15, table 1) containing phenocrysts of plagioclase (5-20%, 2-4 mm), clinopyroxene (trace-3%, 2-4 mm), orthopyroxene (trace-3%, 1-4 mm), and olivine (0-trace) in a cryptocrystalline to pilotaxitic groundmass. Whole rock ⁴⁰Ar/³⁹Ar mean age of andesite (loc. E, table 3) is 0.58±0.03 Ma.

Qlb Breccias. Massive, structureless carapace(?) breccias containing angular to subrounded clasts as much as 3 m in diameter. Rock is similar to associated dome rock (Qld), but typically has been

altered and iron oxide-stained by hydrothermal fluids.

Flat Top eruptive center (Pleistocene)—

Vent area forms conspicuous Flat Top peak on southwest side of Akutan Volcano. Lava flows overlies ancestral Akutan lava flows (unit Qaa). Rocks are orthopyroxene-free, similar to rocks from most other satellite centers.

Qfd Dikes. Basalt(?) dikes, as much as 2 m wide, radiate from vent area.

Qfb Vent breccia complex. Together with plugs (Qfp) forms steep-sided, erosion resistant peak. No samples collected.

Qfp Volcanic plugs. Massive, basalt(?) plugs in vent breccia complex.

Qfl Lava flows. Thin (2 m) to medium (6 m) (at distal ends) lava flows exhibiting conspicuous reddish, oxidized scoriaeous tops and bottoms. Rocks are medium gray to medium dark gray porphyritic basalts (50.3-51.3% SiO₂, loc. 16 and 17, table 1) containing phenocrysts of plagioclase (10-20%, 3 mm), olivine (2-6%, 1-2 mm), and clinopyroxene (trace-3%, 0.5-1 mm) in an intergranular groundmass. Whole rock ⁴⁰Ar/³⁹Ar mean age of basalt (loc. G, table 3) is 0.25±0.04 Ma. Unit as mapped may include flows from both present Akutan Volcano and ancestral Akutan.

Cascade Bight eruptive center

(Pleistocene)—Vent area forms dark, conspicuous, unnamed peak on the southeast side of Akutan Volcano. Rocks tend to be more silicic than those from neighboring Flat Top eruptive center.

Qcd Dikes. At least two dikes, as much as 3 m thick, intrude the Cascade Bight vent breccia complex (Qcb). Rocks are medium dark gray, porphyritic basaltic andesites containing phenocrysts of plagioclase (8-12%, 4 mm), clinopyroxene (2-5%, 3 mm), and olivine (<1%, <1 mm) in a cryptocrystalline groundmass.

- Qcb Vent or cone breccias. Chiefly reddish scoria and cinder mixed with massive blocky lava.
- Qcp Plugs. Massive spires with vertical walls as much as 30 m high. Rocks not sampled.
- Qcl Lava flows. Thin (2-5 m thick) lava flows, exhibiting reddish scoriaceous tops and bottoms, dip away from summit breccia and plug area. Rocks are medium dark gray porphyritic basaltic andesites (55.1% SiO₂, loc. 18, table 1) containing phenocrysts of plagioclase (10-15%, 3 mm), clinopyroxene (1-5%, 3 mm), orthopyroxene (1-3%, 1 mm), and olivine (1-3%, 3 mm) in a cryptocrystalline groundmass. Whole rock ⁴⁰Ar/³⁹Ar mean age of basaltic andesite (loc. H, table 3) is 0.15±0.05 Ma.

Smaller satellite centers (Pleistocene)—

Remnants of at least three cinder cones that have been modified by erosion overlies lava flows (Qaa) from ancestral Akutan Volcano. One cone, containing a central plug, is probably the source of a trachyte dike that is the most silicic rock known to be associated with Akutan Volcano.

- Qcc Cinder cone. Chiefly reddish scoria cinder, and bombs.
- Qccp Plug. Massive lava plug within cinder cone. Rock is a medium dark gray, porphyritic andesite or dacite containing phenocrysts of plagioclase (10-15%, 3 mm) and clinopyroxene (5-10%, 3 mm) in a pilotaxitic groundmass.
- Qccd Dike. Light-colored dike up to 7 m wide, that appears to originate in cinder cone (Qcc) and extend more than 2 km southwest to Open Bight valley. Rock is a light brownish-gray, porphyritic trachyte (67.8% SiO₂, loc. 19, table 1) containing phenocrysts of plagioclase (5-10%, 3 mm), orthopyroxene (2-5%,

1.5 mm) and clinopyroxene (1-2%, 1.5 mm) in a trachytic groundmass containing 1-2% opaque minerals.

Akutan Island Volcanic and Intrusive Rocks

Includes all lava flows and volcaniclastic deposits exposed over the eastern half of the island. Dashed line, which roughly coincides with the 1000-foot elevation contour, approximately separates subaerial volcanic rocks (above) from subaqueous volcanic rocks (below). This change from subaqueous to subaerial deposition has been the basis in earlier studies (Swanson and Romick, 1988; Romick and others, 1990; Romick, 1991), for dividing the rocks of eastern Akutan Island into the Hot Springs Bay volcanics (subaqueous) and the Akutan volcanics (subaerial). Many of the volcanic rocks are undoubtedly related to ancestral Akutan Volcano (Qaa). Others were erupted from scattered local centers, and still others are from unknown sources, some of which are offshore the present island. The pronounced change in eruption environment from subaqueous to subaerial indicates a significantly higher stand of sea level prior to the construction of ancestral Akutan volcano, which probably began during early Pleistocene time.

Intrusive rocks (Holocene(?), Pleistocene and Pliocene)

QTdi Dikes, undifferentiated. Chiefly andesitic to basaltic in composition. Dikes on east and northeast parts of island tend to strike northwesterly subparallel to fault orientation. Dikes on west and southwest parts of island are more varied in orientation and tend to radiate from the Akutan summit area. Dikes exposed in sea cliffs are largely plotted from aerial observations and most have not been examined on the ground. Not all dikes are shown on map.

QTg Gabbro. Small pluton of fine-to-medium-grained equigranular gabbro (51.7% SiO₂, loc. 20, table 1) intrusive into subaqueous volcanic rocks (QTV) in Hot Springs Bay. Pluton is highly fractured and hydrothermally altered; disseminated pyrite is locally abundant. Rock consists of plagioclase (75-90%) and interstitial clinopyroxene (10%) and olivine? (5%).

Extrusive rocks (Pleistocene and Pliocene)

QTd Domes. Domes or massive flows generally associated with small subaqueous cinder cones (QTC). Rocks exhibit spectacular columnar joints. They are greenish-black to medium gray, porphyritic basalts (50.3-51.6% SiO₂, loc. 21, 22, and 23, table 1) containing phenocrysts of plagioclase (5-15%, 3-4 mm), clinopyroxene (1-10%, 2-3 mm), and olivine (trace-3%, 1-2 mm) in a pilotaxitic groundmass. Whole rock ⁴⁰Ar/³⁹Ar mean age of the basalt (loc. C, table 3) is 1.55±0.04 Ma.

QTC Cinder cones. Stratified and typically palagonitized cinder, scoria, and bombs.

QTV Volcanic rocks, undifferentiated. Above about 1000 feet in elevation, chiefly subaerial lava flows with interlayered lahars and airfall tuffs. Below about 1000 feet in elevation, chiefly subaqueous volcanic rocks including pillow

lavas, pillow lava breccias, highly contorted and stubby columnar-jointed flows, monolithic and heterolithic debris flows, pyroclastic flows, and volcanic gravel and boulder deposits. Both subaerial and subaqueous rocks are mainly dark gray to olive black olivine basalts and basaltic andesites (48.5-53.3% SiO₂, loc. 24, 25, 26, 27, table 1) that exhibit textures ranging from aphanitic to highly porphyritic. Porphyritic varieties contain phenocrysts of plagioclase (5-40%, 3-6 mm), olivine (1-10%, <1-3 mm), and clinopyroxene (0-15%, 2-3 mm) in pilotaxitic to intergranular groundmasses. A whole rock ⁴⁰Ar/³⁹Ar isochron age for a basaltic andesite (loc. A, table 3) is 3.29±0.11 Ma and a whole rock ⁴⁰Ar/³⁹Ar mean age for a basalt(?) (loc. B, table 3) is 2.34±0.07 Ma. A unique submarine pyroclastic flow or debris flow, that is exposed in the sea cliffs between Talus Point and Green Bight, contains clasts of nonhydrated rhyolitic obsidian (72.5% SiO₂, loc. 28, table 1) as much as 15 cm in diameter. Primary layering attitudes in the deposit and enclosing rocks indicate an offshore source to the south or southeast. Other subaqueous deposits that may have offshore sources are exposed along the south side of Akutan Harbor, in the Akutan Point area, and around Hot Springs Bay.

USGS LIBRARY - RESTON



3 1818 00265865 4